0026-895X/02/6203-514–520$7.00
MOLECULAR PHARMACOLOGY
Vol. 62, No. 3
1579/1006083
Mol Pharmacol 62:514–520, 2002
Printed in U.S.A.

Identification of Interaction Sites of Cyclic Nucleotide Phosphodiesterase Type 3A with Milrinone and Cilostazol Using Molecular Modeling and Site-Directed Mutagenesis

W. ZHANG, H. KE, and R. W. COLMAN

The Sol Sherry Thrombosis Research Center, Temple University School of Medicine, Philadelphia, Pennsylvania (W.Z., R.W.C.); and Department of Biochemistry and Biophysics and Lineberger Comprehensive Cancer Center, University of North Carolina at Chapel Hill, North Carolina (H.K.)

Received December 28, 2001; accepted April 29, 2002

This article is available online at http://molpharm.aspetjournals.org

ABSTRACT

To identify amino acid residues involved in PDE3-selective inhibitor binding, we selected eight presumed interacting residues in the substrate-binding pocket of PDE3A using a model created on basis of homology to the PDE4B crystal structure. We changed the residues to alanine using site-directed mutagenesis technique, expressed the mutants in a baculovirus/Sf9 cell system, and analyzed the kinetic characteristics of inhibition of the mutant enzymes by milrinone and cilostazol, specific inhibitors of PDE3. The mutants displayed differential sensitivity to the inhibitors. Mutants Y751A, D950A, and F1004A had reduced sensitivity to milrinone (K_i changed from 0.66 μM for the recombinant PDE3A to 7.5 to 156 μM for the mutants), and diminished sensitivity to cilostazol (K_i of the mutants were 18- to 371-fold higher than that of the recombinant PDE3A). In contrast, the mutants T844A, F972A and Q975A showed increased K_i for cilostazol but no difference for milrinone from the recombinant PDE3A. Molecular models show that the PDE3 inhibitors cilostazol and milrinone share some of common residues but interact with distinct residues at the active site, suggesting that selective inhibitors can be designed with flexible size against PDE3 active site. Our study implies that highly conserved residuals Y751, D950 and F1004 in the PDE families are key residues for binding of both substrate and inhibitors, and nonconserved T844 may be responsible for the cilostazol selectivity of PDE3A. Detailed knowledge of the structure of inhibitory sites should contribute to development of more potent and specific inhibitory drugs.

Inhibition of platelet activation is a fundamental step in prevention and treatment of cerebral ischemia/thrombotic disorders and cardiovascular diseases. The endothelial autocrine mediators nitric oxide and prostacyclin are physiologically platelet-inhibitory activation compounds and elevate intracellular cGMP and cAMP levels, respectively. cGMP-inhibited cAMP phosphodiesterase (PDE3A), the most abundant form of cyclic nucleotide phosphodiesterase (PDE) in platelets, hydrolyzes cAMP and lowers its intracellular content. Inhibitors of PDE3A serve as potent antiplatelet agents. Although aspirin, an irreversible inhibitor of platelet cyclooxygenase activity (Hidaka and Asano, 1976), and ticlopidine or clopidoprel, specific inhibitors of ADP-stimulated platelet function (Mills et al., 1992), are standard antiplatelet drugs with proven efficacy in secondary prevention of stroke and myocardial infarction, they fail to alter the pathologic impairment of hemostasis in cardiopulmonary bypass, because they are unable to inhibit thrombin-induced platelet activation. In contrast, the elevation of cAMP blocks all signal transduction pathways in platelets, including the responses to thrombin. Inhibitors of PDE3A, increasing intracellular cAMP and synergizing with nitric oxide in platelet (Hidaka and Endo, 1984), have shown potential application in modulation of coronary artery reocclusion, which occurs in up to one third of patients who undergo angioplasty or thrombolytic therapy.

Currently, two PDE3 type-selective inhibitors are used in clinical practice. One, cilostazol, with antiplatelet, antithrombotic, and vasodilatory effects, has been approved for the treatment of patients with intermittent claudication (Dawson, 2001) and for prevention of short- and medium-term vessel closure as well as late restenosis after intracoronary stenting (El-Beyrouty and Spinler, 2001; Tanabe et al., 2001). The other, milrinone, improves the hemodynamic status of heart failure via inotropic/vasodilatory effects attributable to the increase in cardiac intracellular cAMP level (Kishi et al., 2001). Milrinone is used for the treatment perioperative severe heart failure or marked deterioration of congestive heart failure (Kikura and Levy, 1995).

The three-dimensional atomic structure of the catalytic

This work was supported by National Heart, Lung, and Blood Institute program project grant P01-HL64943 (R.W.C.) and National Institutes of Health grant R01-GM59791 (H.K.).

ABBREVIATIONS: PDE, phosphodiesterase.

domain of PDE4B2B has been recently determined (Xu et al., 2000) and provides considerable insight into the mechanism of catalysis and specificity of PDE4 and other PDE families. In a previous study (Zhang et al., 2001), we constructed a molecular model of the catalytic portion of human platelet PDE3A complex with substrate based on the homology to the X-ray crystal structure of PDE4B and the data from site-directed mutagenesis of PDE3A. The visualized image for interactions between the enzyme active site and substrate cAMP or cGMP was presented by that study. However, to identify PDE3 inhibitor binding sites and mechanisms of inhibition, to facilitate the development of more potent and selective PDE3 inhibitors, and to visualize the nature of the molecular contacts between various inhibitors and PDE3A, more detailed knowledge of interactions between inhibitors and the enzyme is required. In the present study, we select and mutate presumed interacting amino acids in the catalytic clefts of PDE3A, characterize the properties of selected mutants using the PDE3-selective inhibitors cilostazol and milrinone, and generate models of the inhibitor-enzyme complex of PDE3A according to the data from mutagenesis and the homology model of the enzyme-substrate complex of PDE3A.

Materials and Methods

Materials. Protease inhibitors pepstatin, leupeptin, benzamidine, soybean trypsin inhibitor, tosyl phenylalanyl chloromethylketone, cAMP, cGMP, and milrinone were purchased from Sigma-Aldrich (St Louis, MO). [^{3}H]cAMP was from Amersham Biosciences (Piscataway, NJ). Cilostazol was provided by Otsuka Pharmaceutical Co (Rockville, MD).

Generation of a Human Platelet PDE3A Expression Plasmid. A vector pBSPDE3.3 (Cheung et al., 1996) contains nucleotides from 1993 to 3841 of the human platelet PDE3A (GenBank accession number U36798) was digested by *Xho*I and *Sac*I. This DNA fragment, which covers the catalytic portion of the human platelet PDE3A, was subcloned to a pCR 2.1 vector through *Xho*I and *Sac*I sites (Invitrogen, Carlsbad, CA). Because there is a *Kpn*I site right after *Sac*I in pCR 2.1 vector, a clone with the insert was completely digested with *Xho*I and *Kpn*I to add a *Kpn*I site at the 3′end of PDE3A for cloning purposes. The 2-kb *Xho*I-*Kpn*I DNA fragment, which covers the entire catalytic region of PDE3A, was then cloned to the baculovirus expression vector pBlueBacHis 2 (Invitrogen, Carlsbad, CA) to generate pBBH3031. This vector contained an extra oligonucleotide fragment for 31 amino acids, including six histidines and an enterokinase cleaving site. When expressed, the specific activity was similar to that of the enzyme expressed in yeast or purified from platelets (Cheung et al., 1996).

Site-Directed Mutagenesis. All mutagenic oligonucleotide primes were obtained from Invitrogen (Carlsbad, CA). Site-directed mutagenesis of the recombinant PDE3A was performed with a QuikChange site-directed mutagenesis kit (Stratagene, La Jolla, CA).

Expression in Baculovirus/Sf9 Cell System and Purification of a Recombinant PDE3A and Mutants. All procedures were described in detail previously (Zhang and Colman, 2000; Zhang et al., 2001). Briefly, Sf9 cells were maintained in Grace's insect medium with supplements (lactalbumin hydrolysate, L-glutamine, TC-yeastolate) and 10% fetal bovine serum at 27°C. Sf9 cells were cotransfected with Bac-N-Blue DNA, a linearized AcMNP virus DNA (Invitrogen), and the expression vector pBBH3031 or the vector pBBH3031 containing a desired mutation. Cotransfection was carried out by the lipofection method (insect transfection kit from Invitrogen). For expression 5×10^7 cells were infected at an infection multiplicity of 6 in a T-75 flask. The cells were collected 96 h after infection. Preparation and purification of the recombinant virus and the mutated viruses were performed according to the protocol from Invitrogen. The Sf9 cells were harvested 4 days after the virus infection. The cells were collected by centrifugation at 3,000*g* for 15 min, rinsed by in 0.1 M sodium phosphate butter containing 0.15 M NaCl at pH 7.4, and resuspended in lysis buffer (50 mM Tris-HCl, pH 7.8, 10 mM $MgCl_2$ with 0.5 μg/ml pepstatin, 0.5 μg/ml leupeptin, 2 μM benzamidine, 10 μg/ml soybean trypsin inhibitor, and 50 μM tosyl phenylalanyl chloromethylketone). The cells were disrupted with a sonicator probe at 30 spare pulses for a total time of 2 min in ice. Cell debris was removed by centrifugation at 15,000*g* for 30 min at 4°C. The supernatant was either stored at −80°C or further purified. ProBond nickel-chelating resin was used for the protein purification; 1 ml resin was first washed with a binding buffer (50 mM Tris-HCl, pH 8.0, 0.5 M NaCl, and 25 mM imidazole), mixed with 2 ml of supernatant of the cell lysate and 8 ml of the binding buffer, and then rotated for 20 min. The resin was washed three times with the same binding buffer and packed in a 10-ml column. The PDE3A protein was eluted by the elution buffer (50 mM Tris-HCl, pH 7.0, 0.5 M NaCl, and 250 mM imidazole), and fractions were collected. The purified proteins were further dialyzed against 50 mM Tris-HCl, pH 7.8, 10 mM $MgCl_2$, and 20% glycerol. All procedures were done at 4°C. Protein concentrations in cell lysates, were determined by Coomassie Brilliant Blue Protein Assay Reagent (Bio-Rad) with bovine serum albumin as a standard.

PDE Activity Assay. Enzymatic activity was measured as described previously (Zhang et al., 2001). Briefly, in a total volume of 0.1 ml containing 50 mM Tris-HCl, pH 7.8, 10 mM $MgCl_2$, and [^{3}H]cAMP (40,000 cpm/assay) at 24°C for 30 min. The reactions were terminated by addition of 0.2 ml of 0.2 M $ZnSO_4$ and 0.2 ml of 0.2 M $Ba(OH)_2$. The samples were vortexed and spun at 10,000*g* for 3 min. The labeled product of the reaction [^{3}H]5′-AMP was precipitated with $BaSO_4$, and the unreacted [^{3}H]cAMP remained in the supernatant. Radioactivity in the supernatant was determined by liquid scintillation counter. V_{max} and K_m values were calculated by Lineweaver-Burk plots with eight concentrations of cAMP from 0.04 to 20 μM using Microsoft Excel (Microsoft Corp., Redmond, WA). The values of K_{app} were calculated by double reciprocal plots at six concentrations of substrate cAMP and in presence of five different concentrations of each inhibitor as well as without inhibitor. The K_i for recombinant PDE3A and all mutants were determined by replotting the values of K_{app} versus the concentrations of each inhibitor.

Models of Inhibitor-Enzyme Complexes of PDE3A in the Catalytic Portion of PDE3A. The catalytic domain of PDE3A was modeled on basis of the PDE4B structure, as described previously (Zhang et al., 2001). The binding location of the PDE3A inhibitors was simulated according to the crystal structure of PDE4D-rolipram (Q. Huai, H. Wong, H. Y. Kim, Y. Liu, and H. Ke, unpublished observations). The models for cilostazol and milrinone were manually built into the active site of PDE3A using program O (Jones et al., 1991) and the binding was optimized using the program CNS (Brunger et al., 1998). The conformation of the inhibitors was adjusted in accordance to the mutagenesis data.

Results

Selection of Inhibitors. Two PDE inhibitors, milrinone (1,6-dihydro-2-methy-6-oxo-3,4-bipyridine-5-carbonitrile) and cilostazol (l 6-[4-(1-cyclohexyl-1H-tetrazol-5-yl)butoxy]-3,4-dihydro-2(1H)-quinolinone) were used to study interactions with PDE3A. Milrinone and cilostazol are PDE3-specific inhibitors. Both of them have been approved by the United States Food and Drug Administration and are used in clinical treatment. The former is prescribed in patients with severe heart failure (Kikura and Levy, 1995; Kishi et al., 2001); the latter is used in patients with intermittent claudication (Beebe et al., 1999). The

potency of inhibition of milrinone and cilostazol on PDE3A is similar, although these two drugs differ substantially in their chemical structures.

Selection of Mutagenesis. As competitive inhibitors, milrinone and cilostazol should directly compete with the substrates for the binding site in the active site of PDE3A. Our data are consistent with a competitive inhibitory mechanism for both milrinone and cilostazol (Robertson et al., 1987). Fig. 1 shows that double reciprocal plots for the recombinant PDE3A at various concentrations of milrinone and cilostazol intersect at $1/V_{max}$. Because cAMP and cGMP are substrates of PDE3A, the structure of the PDE3A catalytic domain was used to probe the inhibitor interaction sites. In a previous study (Zhang et al., 2001), we identified the overlapping but distinct cAMP and cGMP substrate binding sites with PDE3A and generated a molecular model of the PDE3A catalytic domain. Five amino acids were selected to mutate to alanine in the present study based on the amino acids interacting with the cAMP and cGMP substrate binding sites. We also used our previous model of the cAMP and cGMP binding sites and manually docked the structure of cilostazol as shown in Fig. 2. We added three additional amino acids that seemed sufficiently close to cilostazol to potentially interact for a total of eight amino acids. Mutation, expression, and purification of the recombinant PDE3A and mutants were carried out as described previously (Zhang and Colman, 2000; Zhang et al., 2001).

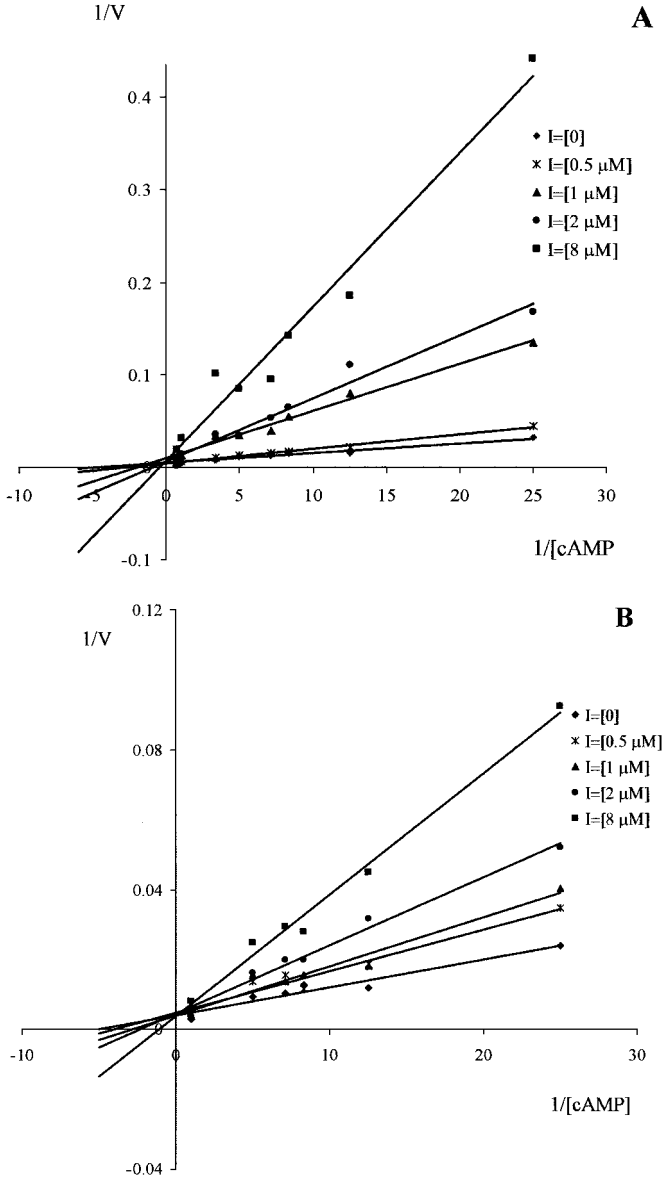

Fig. 1. Inhibition of recombinant PDE3A by cilostazol and milrinone. Double-reciprocal Lineweaver-Burk plots derived from kinetic curves are shown. The assays were performed as described under *Materials and Methods*. A plot of a typical measurement out of three determinations is depicted. Milrinone (A) and cilostazol (B) behave as competitive inhibitors for recombinant PDE3A.

Characterization of Sensitivity of PDE3A Mutants. The K_i values of milrinone (Fig. 3A) and cilostazol (Fig. 3B) for the recombinant PDE3A are 0.66 and 0.57 μM, respectively. Despite the similar K_i values for the two inhibitors, the amino acids that contribute to interaction with each of the inhibitors are different. Six mutants (Y751A, T844A, D950A, F972A, Q975A, and F1004A) show increased K_i with cilostazol, but only three mutants (Y751A, D950A, and F1004A) show increased K_i with milrinone (Table 1). Mutant F1004A has the largest changes in K_m for cAMP and K_i for cGMP that correlate with the large changes in K_i for milrinone as well as cilostazol. The data indicate that F1004 participates directly in the binding of substrate and both selective inhibitors. The mutants Y751A and D950A showed large changes in K_i for cGMP and also significant changes in values of K_i for either milrinone or cilostazol, suggesting that these amino acids are involved in binding of cGMP and the selective inhibitors. The mutants T844A and Q975A have normal range of K_m for cAMP and K_i for cGMP but significantly increased K_i values for cilostazol, suggesting that these residues preferentially interact with the inhibitor.

Integration of Mutagenesis Data Into the Molecular Model of PDE3A. In the milrinone model, milrinone stacks over F1004 and forms two hydrogen bonds with D950, and a hydrogen bond with Y751 (Fig. 4A). This binding is ready to interpret the mutagenesis data that mutation of Y751A, D950A, and F1004A increased K_i by 11-, 18-, and 236-fold, respectively. Milrinone has weak hydrophobic interactions with F972 and no interaction with T844, N845, L910, and Q975. This milrinone model is compatible with the mutagenesis data that the change of the residues to alanine showed little impact on the K_i values (Table 1).

Cilostazol forms a hydrogen bond with residue D950, and exhibits van der Waals interaction with residues Y751, T844, F972, Q975, and F1004 (Fig. 4B). This binding of cilostazol accounts for the 13- to 371-fold increase of K_i when these residues are mutated to alanine. No interactions were found between cilostazol and N845 and L910. This result also corresponds well with no change of the K_i of the mutants (Table 1).

Both cilostazol and milrinone bind three common residues Y751, D950, and F1004. Interestingly, these three residues were also proposed as the key residues for the binding of cAMP and cGMP (Zhang et al., 2001). Because these residues are conserved across all 11 families of PDE, we propose that these three residues may not only serve as key residues for substrate binding and catalysis but also play important roles for inhibitor binding in all families of PDE. On the other hand, cilostazol shows much more direct interactions with PDE3A residues than milrinone, indicating a different bind-

ing mode of two inhibitors. The comparison of the binding of the two inhibitors implies that more potent inhibitors with various sizes and components may be designed against the same active site of PDE.

Discussion

A molecular model of substrate cAMP or cGMP with PDE3A has been generated in our previous study (Zhang et al., 2001). In this model, the phosphate portion of cAMP is located next to Zn^{2+} and forms hydrogen bonds with H752 as well as the Zn^{2+} binding residues of D837 and D950. The sugar group of cAMP forms van der Waals interaction with Y751, L910, and I968, whereas the adenine ring of cAMP interacts with hydrophobic residues of D972, D989, and D1004. The targeted sites by the inhibitors should be at least partially in the substrate binding sites or close to it, because milrinone and cilostazol are competitive inhibitors, as revealed by the data of kinetic studies. Eight amino acids tested in this study were chosen based on this presumption.

Y751 is a conserved amino acid in all PDE families except phenyalanine in PDE9. We have shown previously that although the catalytic efficiency of mutant Y751A is only 5.6% of the recombinant PDE3A, the K_m for cAMP is only increased by 2.5-fold. This result indicates that Y751 is more involved in the catalytic mechanism rather than in cAMP binding. Mutation of Y751 to A in PDE3A leads to 15-fold increase of K_i for cilostazol and 9-fold increase for milrinone. These values are similar to the K_i for the competitive inhibitor cGMP which exhibits a 9-fold increase in K_i for the mutant Y751A. The mutagenesis results agree well with the molecular models of inhibitor-PDE3A complexes, where Y751 interacts with cilostazol and forms a hydrogen bond with milrinone. The results from other investigators show that the mutation of tyrosine to phenylalanine in the corresponding amino acid of PDE5 results in a 4-fold increase in IC_{50} for zaprinast, whereas the exchange of the tyrosine to alanine leads to 7-fold decrease IC_{50} for this specific PDE5 inhibitor (Turko et al., 1999). Therefore, stack interaction between the tyrosine residue and the inhibitor zaprinast in PDE5 is implied. On the other hand, the mechanism of hydrogen bond interactions between the corresponding tyrosine residue in PDE4 and a PDE4-specific inhibitor rolipram was proposed based on the presumption of a peptide model of PDE4 (Polymeropoulos and Hofgen, 1999). The site-directed mutagenesis data further sustain this assumption because replacement of the corresponding tyrosine of PDE4 to phenylalanine causes a 1000-fold increase in IC_{50} for rolipram (Atienza et al., 1999). Taken together, conserved amino acid residues in all PDE gene families are putative targets for PDE-type specific inhibitors; however, the mechanisms of interactions among type-specific inhibitors and individual PDE enzymes widely vary.

There are 20 conserved amino acid residues in PDE families; some of them are critical to enzymatic catalysis. D950 in PDE3A is one of them. Mutation of D950 to alanine in PDE3A results in 99% loss in the catalytic efficacy, whereas mutation of this conserved aspartic acid to alanine in PDE5 also leads to loss 99% catalytic capacity (Turko et al., 1998). In this study, we found that D950 in PDE3A is a contact site with its specific inhibitors. Mutant D950A lost its sensitivity to milrinone and cilostazol, as shown by the 18- and 21-fold increase of K_i for milrinone and cilostazol, respectively. This change in K_i is similar to the 53-fold increase in cGMP, but the K_m for cAMP is not affected in the mutant. Both inhibitors form hydrogen bonds with D950 in the molecular models of the inhibitor-PDE3A enzyme complexes. Furthermore,

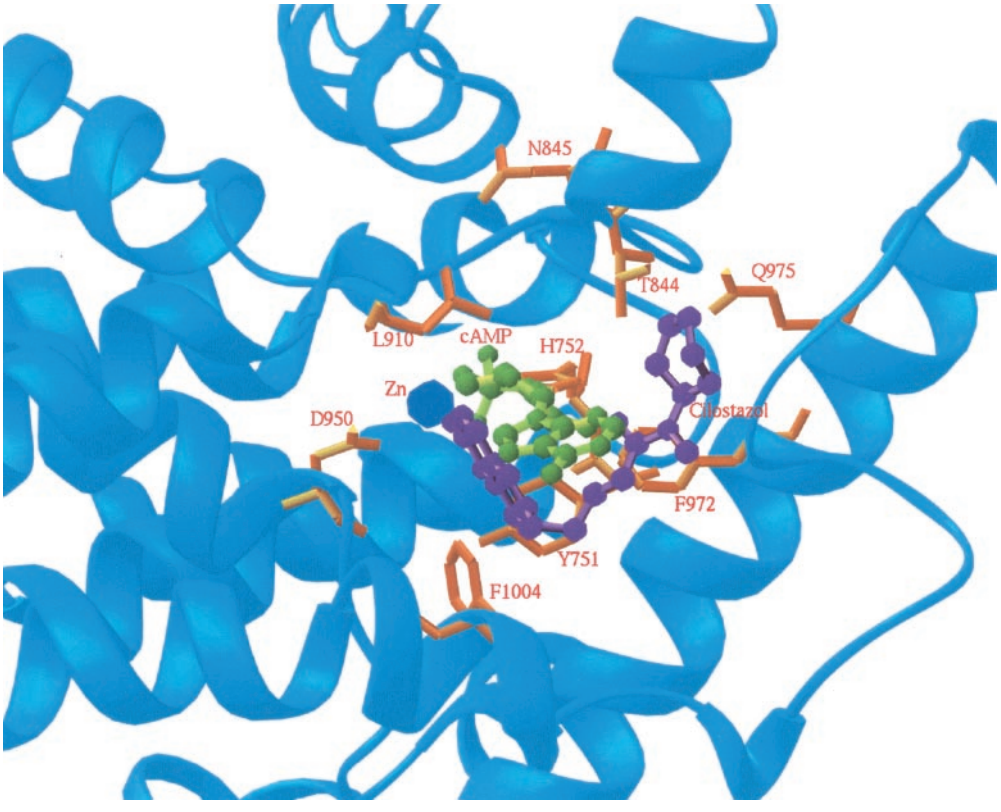

Fig. 2. Relative positions of eight mutated amino acids with substrate cAMP and inhibitor cilostazol. cAMP and cilostazol are colocated in the active site cleft of PDE3A. PDE3A is presented as ribbons. Eight amino acids are shown as brown sticks, cAMP molecules are represented as small green balls and cilostazol as purple balls. Zinc is a blue hexagon.

Turko et al. (1998) reported that substitution of D754 to alanine in PDE5 (corresponding to D950 in PDE3A) led to a 43-fold increase of IC_{50} for zaprinast. These observations suggested that some conserved catalytic residues in PDE families such as D950 participate in interactions with type-specific inhibitors.

Six amino acid residues (Y751, T844, D950, F972, Q975, and F1004) are identified as potential inhibitor binding partners. Most of them are either substrate cAMP binding sites, substrate cGMP binding sites, or both. F1004 in PDE3A is recognized as substrate cAMP and cGMP binding sites (Zhang and Colman, 2001; Zhang et al., 2001). Mutant F1004A leads to a 100-fold increase of K_i values for milrinone, cilostazol, and cGMP, and a 100-fold increase in K_m for cAMP. The mutagenesis data are well consistent with the molecular models. F1004 stacks over milrinone and forms hydrophobic interaction with cilostazol in the molecular models. These observations verify that a competitive inhibition mechanism is involved in inhibitory effects by milrinone and cilostazol in PDE3A. However, some PDE3 selective inhibitor contact sites (T844 and Q975) are in neither the cAMP nor the cGMP binding sites. These data demonstrate that cAMP and cGMP in PDE3A is partially distinct from the milrinone and cilostazol binding sites.

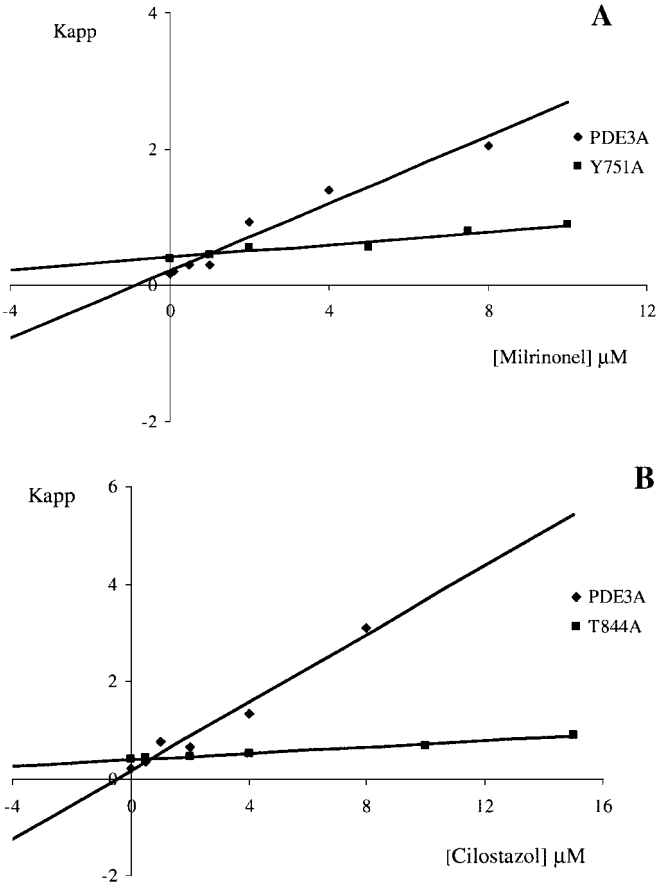

Fig. 3. Determination of the K_i of PDE3A and mutants for cilostazol and milrinone. A, replot of K_{app} against milrinone concentrations for PDE3A and mutant Y751A. B, replot of the K_{app} versus the concentrations of inhibitor cilostazol to determine the K_i of PDE3A and mutants T844A.

One mutant N845A has no effect on the K_i of cilostazol, milrinone, or cGMP; it only moderately increases the K_m for cAMP. The result indicates that the residue of N845 is in a particular area of the active site. Finally, L910 does not interact with any of the inhibitors or cAMP.

Richter et al. (2001) performed site-directed mutagenesis to identify the amino acids interacting with PDE4 inhibitors. They found five amino acids (Y432, H588, Y602, F613, and F645) that influenced inhibition binding to PDE4. Y432, F613, and F645 in PDE4 corresponded to the three identical amino acids in PDE3A, Y751, F972, and F1004. Mutant Y751A and F1004A decrease the binding of both milrinone and cilostazol; however, F972A increases the K_i of cilostazol without affecting that of milrinone. We did not mutate the residue corresponding to H588 or Y602, but it should be noted that in PDE3A, the amino acids at these positions are different: K947 and H961, respectively.

The mutation of H836 and H840 to Ala leads to a loss of catalytic activity of PDE3A (Zhang et al., 2001). Both residues belong to the metal ion-binding motif, which is conserved among all PDEs. Mutants H836A and H840A show a decreased sensitivity for milrinone and cilostazol (data not shown). Although the molecular model of PDE3A did not support direct contact between these amino acids and the inhibitors milrinone and cilostazol, a loss of metal ion binding would lead indirectly to the loss of inhibitor binding. This explanation is further supported by the fact that the exchange of metal binding residue H473 or H477 for serine in PDE4A results in a decrease of the rolipram binding (Jacobitz et al., 1996). We have calculated the catalytic efficiency

TABLE 1

Inhibition effects of PDE3-selective inhibitors on PDE3A mutants

The mutants are listed in order of their position in the sequence. All determinations represent the mean ± S.D. of at least three separate experiments. The bold values are elevated 3-fold compared with recombinant PDE3A. Differences are statistically significantly ($P < 0.001$) using Student's t-test. Values for cGMP K_i, cAMP K_m, and catalytic efficiency are from Zhang et al. (2001).

	K_i			K_m	
	Cilostazol	Milrinone	cGMP	cAMP	Catalytic Efficiency K_{cat}/K_m
		μM			$\mu M/s$
PDE3A	0.57 ± 0.11	0.66 ± 0.12	0.76 ± 0.09	0.21 ± 0.02	8.58
Y751A	**10.4 ± 3.45**	**7.45 ± 1.06**	**6.71 ± 0.60**	0.53 ± 0.03	0.20
T844A	**14.2 ± 3.29**	1.31 ± 0.11	0.46 ± 0.10	0.35 ± 0.02	1.29
N845A	0.77 ± 0.16	0.90 ± 0.26	0.88 ± 0.06	**0.92 ± 0.26**	1.58
L910A	0.64 ± 0.08	1.89 ± 0.41	1.72 ± 0.15	0.50 ± 0.07	0.59
D950A	**12.1 ± 1.20**	**12.2 ± 1.83**	**40.1 ± 2.26**	0.23 ± 0.01	0.08
F972A	**10.4 ± 0.83**	1.67 ± 0.16	1.67 ± 0.07	**0.65 ± 0.10**	0.56
Q975A	**7.23 ± 1.57**	0.77 ± 0.06	0.24 ± 0.02	0.24 ± 0.05	0.88
F1004A	**212 ± 10.6**	**156 ± 15.5**	**>100**	**27.2 ± 0.61**	0.03

for each our mutants. The catalytic efficiency does not seem to correlate well with cAMP binding or cGMP inhibition.

Each family of mammalian PDE possesses its own specific individual inhibitors. However, the determinant for this selectivity has not been clear. Based on our mutagenesis data and the inhibitor binding models, we speculate that the inhibitor selectivity of PDEs might be determined by both different amino acids in each PDE and subtle conformation variation of the active sites. Although a majority of the residues for binding of PDE3A inhibitors are well conserved in all mammalian PDEs, a few distinct amino acids may be sufficient to differentiate the inhibitors. For example, mutation of a nonconserved amino acid T844 to Ala in PDE3A results in a 25-fold increase in K_i for cilostazol but has no effect on the K_i for milrinone or cGMP or the K_m for cAMP in this study. Our data indicate a decisive role of T844 in the selectivity of PDE3A for cilostazol, and are consistent with the argument that unique amino acids in different types of PDE are critical to determine specificity of specific inhibitor (Atienza et al., 1999). On the other hand, the active sites of

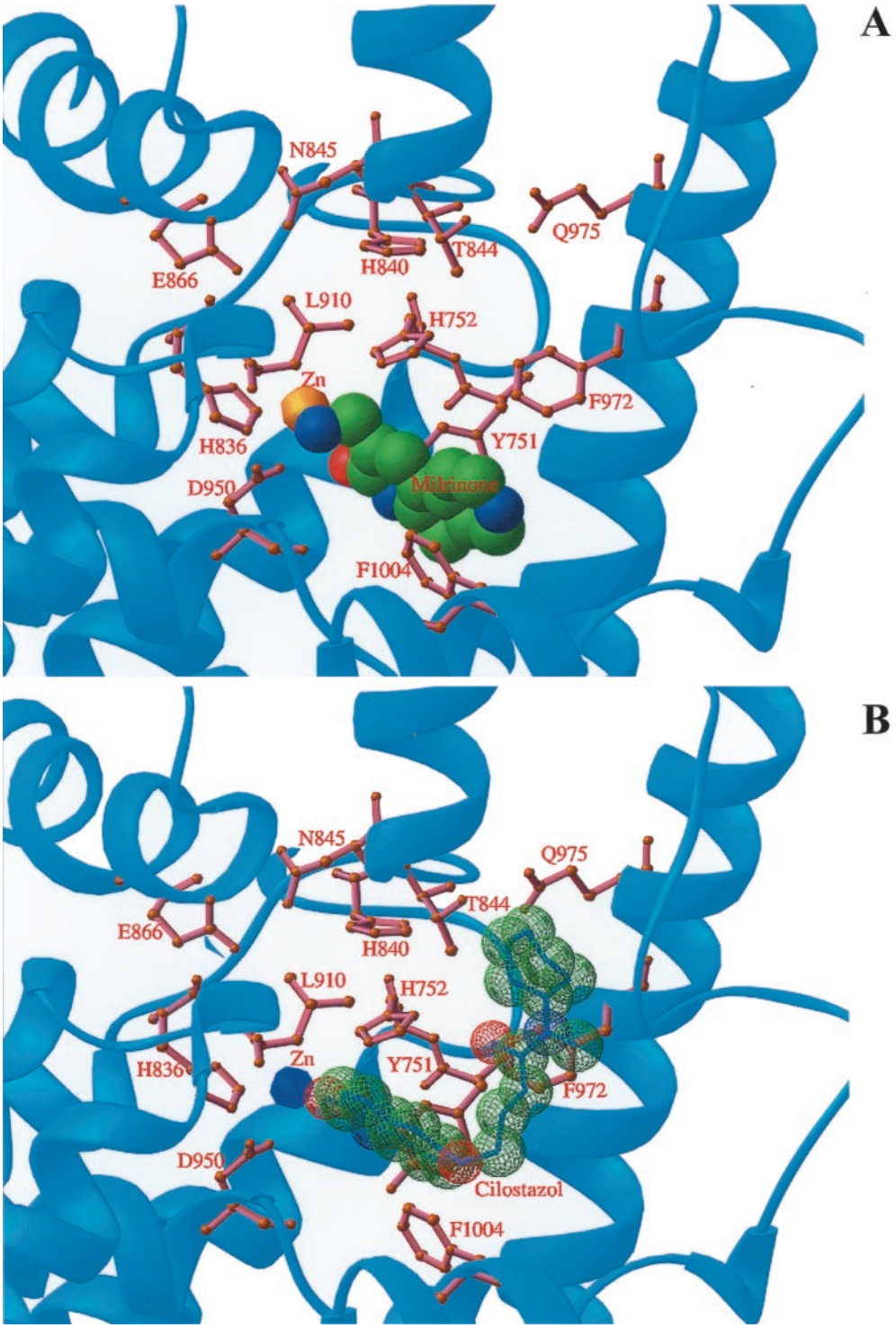

Fig. 4. Binding of milrinone or cilostazol to the active site of PDE3A. PDE3A is shown as ribbons. The PDE3A residues involved in binding are shown as brown sticks and are labeled. Milrinone (A) and cilostazol (B) are represented by large balls; green, carbon atom; red, oxygen atom; blue, nitrogen atom.

PDEs can not only provide various orientations for the inhibitor binding but may also possess subtle different conformations in each PDE family. The conformational difference might thus distinguish and select inhibitors for each family of PDEs, in a key-lock mechanism. However, this argument needs to be verified by the structural studies in the future.

Models of inhibitor-enzyme complexes of PDE3A in the catalytic portion of PDE3A are generated in this study. These models might help us to understand how milrinone or cilostazol bind to and inhibit one of its targets, enzyme PDE3A. Visualization of inhibitor interactions with PDE3A should assist in the development of even better inhibitors.

References

Atienza JM, Susanto D, Huang C, McCarty AS, and Colicelli J (1999) Identification of inhibitor specificity determinants in a mammalian phosphodiesterase. *J Biol Chem* **274:**4839–4847.

Brunger AT, Adams PD, Clore GM, DeLano WL, Gros P, Grosse-Kunstleve RW, Jiang JS, Kuszewski J, Nilges M, et al. (1998) Crystallography & NMR system: A new software suite for macromolecular structure determination. *Acta Crystallogr* **D54:**905–921.

Beebe HG, Dawson DL, Cutler BS, Herd JA, Strandness DE Jr, Bortey EB, and Forbes WP (1999) A new pharmacological treatment for intermittent claudication: results of a randomized, multicenter trial. *Arch Intern Med* 27;**159:**2041–2050.

Cheung PP, Xu H, McLaughlin MM, Ghazaleh FA, Livi GP, and Colman RW (1996) Human platelet cGI-PDE: expression in yeast and localization of the catalytic domain by deletion mutagenesis. *Blood* **88:**1321–1329.

Dawson DL (2001) Comparative effects of cilostazol and other therapies for intermittent claudication. *Am J Cardiol* **87:**19D–27D.

El-Beyrouty C and Spinler SA (2001) Cilostazol for prevention of thrombosis and restenosis after intracoronary stenting. *Ann Pharmacother* **35:**1108–1113.

Hidaka H and Asano T (1976) Platelet cyclic 3′:5′-nucleotide phosphodiesterase released by thrombin and calcium ionophore. *J Biol Chem* **251:**7508–7516.

Hidaka H and Endo T (1984) Selective inhibitors of three forms of cyclic nucleotide phosphodiesterase–basic and potential clinical applications *Adv Cyclic Nucleotide Protein Phosphorylation Res* **16:**245–259.

Jacobitz S, McLaughlin MM, Livi GP, Burman M, and Torphy TJ (1996) Mapping the functional domains of human recombinant phosphodiesterase 4A: structural requirements for catalytic activity and rolipram binding (1996) *Mol Pharmacol* **50:**891–899.

Jones, T. A, Zou, J-Y., Cowan, S. W. & Kjeldgaard, M (1991) Improved methods for building protein models in electron density maps and the location of errors in these models. *Acta Crystallogr* **A47:**110–119.

Kikura M and Levy JH (1995) New cardiac drugs. *Int Anesthesiol Clin* **33:**21–37.

Kishi T, Nakahashi K, Ito H, Taniguchi S, and Takaki M (2001) Effects of milrinone on left ventricular end-systolic pressure-volume relationship of rat hearts in situ. *Clin Exp Pharmacol Physiol* **28:**737–742.

Mills DC, Puri R, Hu CJ, Minniti C, Grana G, Freedman MD, Colman RF, and Colman RW (1992) Clopidogrel inhibits the binding of ADP analogues to the receptor mediating inhibition of platelet adenylate cyclase. *Arterioscler Thromb* **12:**430–436.

Polymeropoulos EE and Hofgen N (1999) *Quant Struct-Act Relat* **18:**543.

Robertson DW, Jones ND, Krushinski JH, Pollock GD, Swartzendruber JK, Hayes JS (1987) Molecular structure of the dihydropyridazinone cardiotonic 1,3-dihydro-3,3-dimethyl-5-(1,4,5,6-tetrahydro-6-oxo-pyridazinyl)-2H-indol-2-one, a potent inhibitor of cyclic AMP phosphodiesterase. *J Med Chem* **30:**623–627.

Richter W, Unciuleac L, Hermsdorf T, Kronbach T, and Dettmer D (2001) Identification of inhibitor binding sites of the cAMP-specific phosphodiesterase 4. *Cell Signal* **13:**287–297.

Tanabe Y, Ito E, Nakagawa I, and Suzuki K (2001) Effect of cilostazol on restenosis after coronary angioplasty and stenting in comparison to conventional coronary artery stenting with ticlopidine. *Int J Cardiol* **78:**285–291.

Turko IV, Francis SH, and Corbin JD (1998) Potential roles of conserved amino acids in the catalytic domain of the cGMP-binding cGMP-specific phosphodiesterase. *J Biol Chem* **273,** 6460–6466.

Turko IV, Ballard SA, Francis SH, and Corbin JD (1999) Inhibition of cyclic GMP-binding cyclic GMP-specific phosphodiesterase (type 5) by sildenafil and related compounds. *Mol Pharmacol* **56:**124–130.

Xu RX, Hassell AM, Vanderwall D, Lambert MH, Holmes WD, Luther MA, Rocque WJ, Milburn MV, Zhao Y, Ke H, et al. (2000) Atomic structure of PDE4: insights into phosphodiesterase mechanism and specificity. *Science (Wash DC)* **288:**1822–1825.

Zhang W and Colman RW (2000) Conserved amino acids in metal-binding motifs of PDE3A are involved in substrate and inhibitor binding. *Blood* **95,** 3380–3386.

Zhang W, Ke H, Tretiakova AP, Jameson B, and Colman RW (2001) Identification of overlapping but distinct cAMP and cGMP interaction sites with cyclic nucleotide phosphodiesterase 3A by site-directed mutagenesis and molecular modeling based on crystalline PDE4B. *Protein Sci* **10:**1481–1489.

Address correspondence to: Dr. Robert W. Colman, The Sol Sherry Thrombosis Research Center, Temple University School of Medicine, 3400 N. Broad Street, Philadelphia, PA 19140. E-mail: colmanr@astro.temple.edu